JOURNAL OF CATALYSIS 99, 349–357 (1986)

Fischer–Tropsch Reaction Studies with Supported Ruthenium Catalysts

II. Effects of Oxidative Pretreatment at Elevated Temperatures

KEVIN J. SMITH*,[1] AND RAYMOND C. EVERSON†,[2]

*Department of Chemical Engineering, University of Natal, Durban 4001; and †Department of Chemical Engineering, Potchefstroom University for CHE, Potchefstroom, 2520, Republic of South Africa

Received August 13, 1985; revised January 6, 1986

The effect of oxidative pretreatment, at elevated temperatures, on the Fischer–Tropsch (FT) synthesis, for a 0.5% Ru on γ-Al_2O_3 catalyst, has been investigated. The FT activity and selectivity of the catalysts was measured for a range of operating conditions using a stirred, gas–solid reactor (Carberry type). The hydrocarbon turnover numbers (TON's) were estimated using a power law correlation of the methane TON, to indirectly estimate the number of active Ru sites during synthesis. The catalyst pretreatment procedure resulted in Ru dispersions between 0.78 and 0.16. The FT higher hydrocarbon (C_5–C_{10}) selectivity and olefinic content of the product increased with the decreased dispersion. The alcohol selectivity, however, did not change significantly with the decreased Ru dispersion. The saturated hydrocarbon specific activities increased with decreased dispersion, indicative of the structure sensitivity of the FT synthesis. The effect of dispersion on the individual hydrocarbon power law parameters (up to C_4) are also reported. With decreased dispersion the activation energies decreased while the magnitude of the H_2 and CO exponents generally increase.

INTRODUCTION

The use of supported Ru for CO hydrogenation to hydrocarbons is well documented (*1–9*). Supported Ru is reported to have a higher Fischer–Tropsch (FT) specific activity than other supported Group VIII metal catalysts (*9*). The higher hydrocarbon selectivity (C_2^+ product fraction) is also greatest on Ru (*9*). Typical results for CO hydrogenation over supported Ru are illustrated by those of Everson *et al.* (*2*) They reported, at suitable reaction pressures (about 800 kPa), temperatures (about 235°C), and conversions, a mainly saturated hydrocarbon product, with a C_5–C_{10} selectivity of about 60 mass%, on a 0.5% Ru/γ-Al_2O_3 catalyst.

For structure-sensitive reactions the specific activity depends on the supported metal crystallite size or metal dispersion. Dalla Betta investigated the synthesis of methane on Ru and Ni and concluded that the activities depended on the metal dispersion (*10*). Magnetic studies on Ni by Everson *et al.* (*11*) confirmed the conclusion. A more detailed study by King (*6*) on supported Ru showed the specific activities for CO consumption and methanation decreased with increasing Ru dispersion. King obtained various dispersions by changing the Ru loading. Recently Kellner and Bell (*4*) have also reported a decreased FT specific activity (C_2^+ and CH_4 production rates) with increased dispersion. Their range of catalyst dispersions were also obtained by changing the catalyst metal loading as well as by sintering under reaction conditions. They observed a decrease in dispersion during an activity measurement and therefore made chemisorption measurements at intervals during their activity measurements. At the end of a reaction period of about 20 min the catalyst was rereduced and its dispersion measured using H_2

[1] Present address: Department of Chemistry, Lehigh University, Bethlehem, Pa. 18015

[2] To whom correspondence should be sent.

0021-9517/86 $3.00

chemisorption. The catalyst dispersion was also estimated *in situ*, using integrated CO IR absorptions. With both techniques they reported the methane specific activity increased with decreasing dispersion.

In the present investigation the effect of high-temperature oxidation on catalyst dispersion for a 0.5% Ru on γ-Al_2O_3 catalyst is reported. The FT activity and selectivity of the sintered catalysts have also been measured for a range of reaction conditions using a stirred gas–solid reactor. A technique to indirectly estimate the number of active sites during FT synthesis is also described, and the effect of crystallite size on FT kinetics is quantified.

EXPERIMENTAL

In the present study a stirred gas–solid reactor, ICI Mark IV (*12*), similar in design to the spinning basket-type reported by Carberry (*13*), was used for kinetic measurements. The experimental system has been described previously (*2*). The absence of external mass or heat transfer effects were confirmed experimentally. For CO conversions less than 95%, and the operating conditions of the present work, the CO conversion remained constant at constant space velocities but varying catalyst loadings. In all cases the reactor stirrer speed was 3500 rpm. Internal diffusion effects were minimal since microprobe studies showed the Ru only penetrated to a maximum depth of 200 μm in the Al_2O_3 support (*7*).

The reaction products were analysed using on-line gas chromatography. A Perkin–Elmer gas chromatograph fitted with dual thermal conductivity and flame ionization detectors was used. Resolution of the component peaks (up to C_{10} hydrocarbons and CO, CO_2, and H_2O) was achieved using a 2-m Porapak Q column with suitable temperature programming. Sample injection was on-line, using a Carle sample valve. Hydrogen was the carrier gas. Hydrocarbons up to C_{10} were resolved within 60 min. Reaction conditions throughout the present investigation were chosen such that the amounts of hydrocarbons formed above C_{10} were small and not detectable. Carbon balances confirmed the absence of significant quantities of hydrocarbons above C_{10} (*7*).

Prior to each experimental run, which lasted approximately 12 h, the reactor was charged with fresh catalyst and inert support for make up of the catalyst-basket volume. The reactor was then heated to 250°C in flowing H_2 (100 sccm, UHP grade, >99.99% purity) and subsequently held at this temperature for a further 2 h for complete catalyst reduction. The reduction temperature of 250°C was chosen on the basis of temperature-programmed reduction (TPR) profiles, obtained for the different catalysts (*7*).

Following the reduction procedure synthesis gas was introduced to the reactor and the required reactor temperature, pressure, and feed gas flow rate set. An initial stabilization period of at least 30 min was allowed before sampling the exist gases.

CATALYSTS AND CATALYST CHARACTERIZATION

The catalysts of the present investigation were 0.5% Ru on γ-Al_2O_3 by mass. The catalysts were supplied by Johnson Mattey (JM) Research Centre (U.K.). Various metal dispersions were obtained by sintering over a range of temperatures for 30 min in air. The sintering procedure in the presence of air did not alter the Ru content of the catalyst which was confirmed by various analyses including measurement of concentration profiles by microprobe analysis. A 0.5% Ru on γ-Al_2O_3 Engelhard (E) catalyst was also included in the present study.

The resulting catalysts were characterized using TPR profiles, measurement of BET surface areas and CO chemisorption, while carbon burnoff estimated the amount of carbonaceous material on the spent catalysts. The TPR profiles of the fresh unreduced catalysts were determined using a 5% H_2 in N_2 gas flowing over the catalyst

while the temperature was programmed linearly at 12°C/min. The resulting profiles showed an optimum reduction temperature of about 250°C for all the catalysts. The CO chemisorption was measured at 100°C. Carbon monoxide pulses were injected into the 100% H_2 gas flow and the CO uptake measured. The stoichiometry of chemisorption was assumed unity, consistent with other reports (*9, 14*). From the chemisorption measurement, the fraction of Ru metal exposed (the Ru dispersion) was calculated. The approximate crystallite size was calculated assuming cubic crystallites using the formula given by Butt (*15*) (see Table 1).

Table 1 summarizes the results obtained for the catalysts of the present investigation. The unsintered catalysts are well dispersed, however, sintering in air for 30 min significantly reduces the dispersion. With a sintering temperature of 500°C the estimated crystallite size increased from 13 to 64 Å.

Catalyst deactivation. Figure 1 shows the methanation rate as a function of time on stream for the unsintered catalysts, at various operating conditions. In all cases the measured rate per gram of Ru decreased significantly in the first 2 h of operation and then reached a fairly constant value for the duration of the run. The observed decrease occurred over a longer time period than anticipated from the system dynamic response, following the introduction of synthesis gas. The decreased activity was presumably due to a loss in active sites, either from sintering or catalyst fouling by carbonaceous deposits.

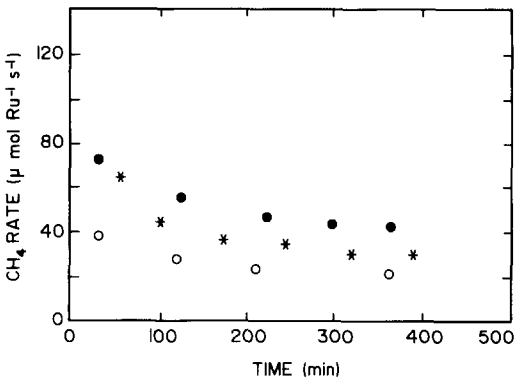

FIG. 1. CH_4 rate as a function of time for the unsintered catalysts: (●) E catalyst at 250°C, 800 kPa, H_2/CO = 3; (○) E catalyst at 235°C, 101 kPa, H_2/CO = 5; (*) JM1 catalyst at 235°C, 800 kPa, H_2/CO = 2.3.

Table 2 shows the measured dispersion and carbon weight percentage on the spent catalysts. For the catalysts operated at H_2/CO = 3, the CH_4 selectivity was about 30 mass%, while with H_2/CO = 5, the CH_4 selectivity was 60 mass%. For the catalysts operated at low H_2/CO ratios (<3/1), the CO chemisorption measurement was not possible because of hydrogenation of the carbonaceous deposits to CH_4, which interfered with the H_2 flow during the measurement.

Table 2 shows that, for H_2CO = 5, the Ru dispersion decreased during a run by about 20%. The carbon burnoff results show that

TABLE 1

Catalyst Characterization Results

Catalyst	Sintering temperature (°C)	BET area (m^2 g^{-1})	Dispersion	Crystallite size[a] (Å)
JM1	—	102	0.78	13
JM7	200	—	0.70	15
JM8	250	—	0.54	19
JM3	300	—	0.47	22
JM6	350	—	0.36	29
JM4	500	—	0.16	64
Engelhard	—	105	0.62	17

[a] Assuming cubic crystallites, with size $l = 6/(S_m\rho)$ where S_m is the metal surface area and ρ = 12.2 g/cm^3. See Refs. (*10, 15*).

TABLE 2

Spent Catalyst Characterization

Catalyst	Reaction conditions			Dispersion	Carbon (mass%)
	H_2/CO ratio	Temp., °C	Press., kPa		
Engelhard		Unreacted		0.62	0.07
JM1		Unreacted		0.78	0.07
Englehard	5/1	250	101	0.47	0.10
Engelhard	5/1	285	101	0.49	0.11
Engelhard	3/1	235	808	—	0.59
JM1	3/1	235	1200	—	1.14

the carbonaceous deposit on the used catalyst was small. Hence the observed decrease in CH_4 rate per gram of catalyst (Fig. 1) is presumably due mainly to the decreased Ru dispersion with a small amount of catalyst fouling (and thus, a loss in active sites) by carbonaceous deposits on the Ru surface. For FT reaction conditions ($H_2/CO < 3$) a much greater increase in carbon burnoff is observed. A decrease in Ru dispersion presumably also occurs.

The above results point to the difficulty in characterising the effective catalyst surface area during FT synthesis. To compare the effects of crystallite properties it is necessary to report synthesis turnover numbers, which require estimates of the number of active sites during synthesis. For high H_2/CO feed ratios ($H_2/CO = 5$ in the present study) the spent catalyst dispersion can be measured and compared with the observed rate after the initial 2 h of synthesis. Since the carbonaceous deposit on the Ru surface for these conditions was small, the average of the unused and spent catalyst dispersions gives a good approximation of the number of active sites during synthesis. For the FT reaction conditions (low H_2/CO feed ratios), however, an indirect method is necessary, details of which will be given presently.

Figure 2 shows the effect of time on stream on the measured hydrocarbon selectivity for a typical set of reaction conditions. It is apparent that the selectivity does not change significantly during the 7 h on stream for the reaction conditions shown.

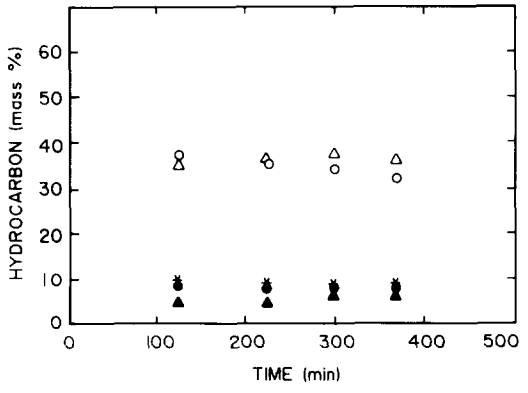

FIG. 2. Hydrocarbon selectivity as a function of time on stream for E catalyst at 250°C, 800 kPa, $H_2/CO = 3$: (△) CH_4; (▲) C_2; (*) C_3; (●) C_4; (○) C_5–C_{10}.

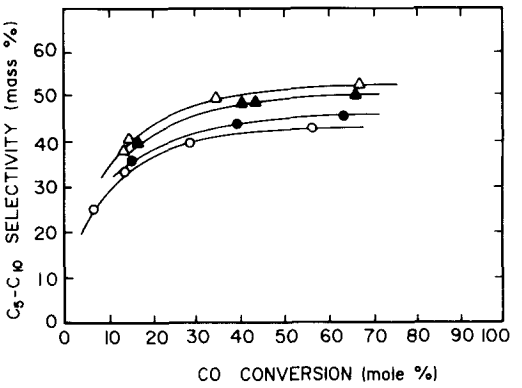

FIG. 3. C_5–C_{10} selectivity as a function of CO conversion of various catalyst dispersions at 235°C, 800 kPa, and $H_2/CO = 2.3/1$: (○) 0.78; (●) 0.70; (▲) 0.47; (△) 0.16.

RESULTS AND DISCUSSION

Production Distributions

The hydrocarbon product distribution was measured for a range of operating conditions for the unsintered and sintered catalysts (*7*). The significant results are summarized in the present paper. Comparisons are based on the fresh catalyst Ru dispersions.

Figure 3 shows the effect of dispersion on the C_5–C_{10} mass% selectivity (defined as the mass% C_5–C_{10} of total product hydrocarbons). Generally, increasing the dispersion decreased the C_5–C_{10} mass% selectivity, irrespective of the conversion. Table 3

TABLE 3

FT Product Distribution as a Function of Ru Dispersion[a]

Catalyst	Dispersion (Fresh catalyst)	CO conv. (%)	C_2^+/C_1 mass ratio	C_5–C_{10} mass %	$C_3^=/C_3$ mole ratio
JM1	0.78	55	3.8	42	0.45
JM7	0.70	63	3.8	45	0.30
JM3	0.47	70	4.7	50	0.73
JM4	0.16	68	5.0	52	1.20

[a] Conditions: temperature 235°C; pressure 800 kPa; $H_2/CO = 2.3/1$.

shows that increased dispersion decreases the C_2^+/C_1 mass ratio and the $C_3^=/C_3$ mole ratio (the latter indicates the unsaturate/saturate hydrocarbon ratio of the product). With an increase in dispersion from 0.16 to 0.78, the $C_3^=/C_3$ mole ratio decreased by a factor of about 3. The rapid decline in olefin–paraffin ratio observed by Kellner and Bell (*4*) for small particle sizes (less than 12 Å) was ascribed to possible support interaction effects. In the present investigation, no such rapid decline was observed. The smallest average particle size for the catalysts of the present investigation was estimated to be 13 Å. Hence support interaction effects do not seem to be important here.

The FT product distribution can be characterized by a probability of growth parameter α, which arises from a polymer chain growth scheme which describes the FT carbon number distribution (*1, 16, 17*). Table 4 shows the observed increase in the parameter with decreasing Ru dispersion, while an example of Anderson–Schulz–Flory type plots are given in Fig. 4.

The results in the present paper differ from other investigations on the structure sensitivity of the FT synthesis on supported Ru. King (*6*) varied the Ru dispersion by changing the catalyst Ru weight loading. Kellner and Bell (*4*) obtained various dispersions with different Ru loadings as well as by sintering under reaction conditions. With dispersions ranging from 0.23 to 0.60

TABLE 4

Probability of Chain Growth as a Function of Ru Dispersion[a]

Catalyst	Dispersion (Fresh catalyst)	C_5–C_{10} Mass %	Probability of growth, α
JM1	0.78	34	0.65
JM7	0.70	33	0.66
JM3	0.47	37	0.67
JM4	0.16	45	0.73

[a] Conditions: temperature 250°C; pressure 1200 kPa; H_2/CO = 2.3/1; CO conv. 22%.

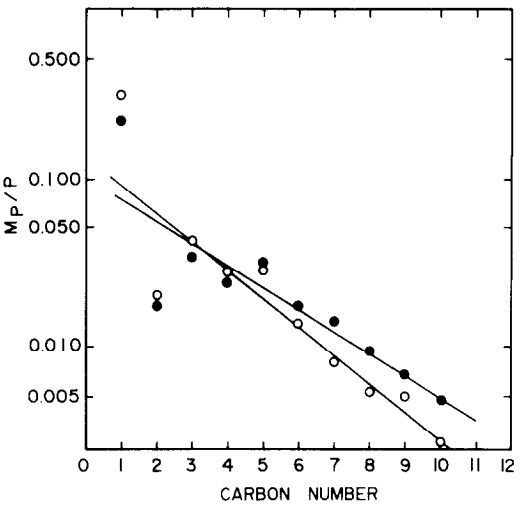

FIG. 4. Anderson–Schulz–Flory plots for JM7 catalyst (○), α = 0.66 and JM4 catalyst (●), α = 0.73 at 250°C, 1200 kPa, H_2/CO = 2.3/1, CO conv.% = 22%. M_p/P is mass fraction of hydrocarbon divided by carbon number.

King observed no consistent change in the C_2^+/C_1 mass ratio. Together with the change in the Ru dispersion, however, the catalyst support pore diameter varied between 137 and 44 Å. Kellner and Bell also report an increase in the probability of chain growth as the Ru dispersion increased from 0.63 to 0.7 (*4*). The reported olefin/paraffin ratio remained fairly constant up to dispersion of about 0.6 and then decreased rapidly. For a similar range of dispersion the $C_3^=/C_3$ ratio of the present investigation, increased with decreasing dispersion, and are about an order of magnitude lower than those reported in (*4*).

For some of the reaction conditions of the present investigation, alcohols (mainly methanol and ethanol) were also produced, a result also reported by Kellner and Bell (*3*). Figure 5 shows the alcohol selectivity (mass% of total product hydrocarbons and alcohols) measured as a function of conversion for the catalysts of the present investigation. The alcohol selectivity does not change significantly with Ru dispersion.

Kinetics

It has been shown that for H_2/CO = 5, the

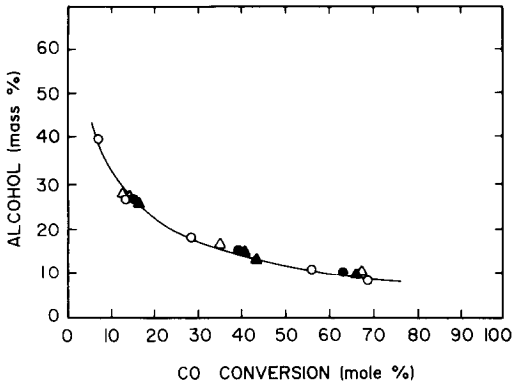

FIG. 5. Alcohol selectivity as a function of CO conversion for various catalyst dispersions at 235°C, 800 kPa, and H_2/CO = 2.3/1: (○) 0.78; (●) 0.70; (▲) 0.47; (△) 0.16.

spent catalyst dispersion was lower than for the fresh catalyst. For $H_2/CO < 3$, the measurement for spent catalyst dispersion was not possible (by the technique used in this investigation) because of the carbonaceous deposit on the catalyst; carbon burnoff's as high as 1.1 wt% were measured on the spent catalyst (Table 2). In determining the FT reaction kinetics in terms of the turnover number TON (mol · (mol. surface Ru)$^{-1}$ s^{-1}) however, an estimate of the effective catalyst surface area during synthesis is required.

To estimate the number of active sites during synthesis, Kellner and Bell made Ru dispersion measurements (by H_2 chemisorption) at various intervals during an experimental run (*4*). The technique is tedious and assumes that the average of the number of Ru sites measured before and after each cycle, corresponds to the actual number active while the synthesis reaction is occurring. They also estimated the Ru dispersion using CO IR integrated absorbances, measured *in situ* at 1010 kPa, 498 K, and H_2/CO = 3. The technique requires an estimate of Ru at the start of the synthesis cycle. The TON's reported by King (*6*), showing the effect of various dispersions on the CO consumption and methane synthesis rates, were based on the Ru dispersions measured on the fresh catalyst. In view of Kellner and Bell's results King's TON's are probably too low.

We propose a different technique for estimating the TON, without making a direct measurement of the Ru dispersion during the course of an experimental run. We assume that the same number of metal sites participate in the synthesis of each hydrocarbon. Hence

$$\frac{r_{c_i}}{r_{c_1}} = \frac{N_{c_i}}{N_{c_1}}$$

where r_{c_i} is the rate of synthesis of hydrocarbon c_i per gram of catalyst and N_{c_i} is the turnover number of hydrocarbon c_i.

In the present work, for synthesis with H_2/CO ratio greater than 3, the spent catalyst Ru dispersion could be measured by CO chemisorption. Hence at such synthesis conditions, N_{C_1} was calculated from the measured rate per gram of catalyst and the measured Ru dispersion. Furthermore the specific methane activity was correlated according to the well-known power rate law:

$$N_{c_1} = k_0 \exp(-E/RT) P_{CO}^a P_{H_2}^b \qquad (1)$$

where a and b are constants and P_{CO}, P_{H_2} the partial pressures of the reactants. Table 5 summarizes the parameter values obtained for the CH_4 TON power law correlation, on the catalyst with fresh catalyst dis-

TABLE 5

Power Law Parameter Values for Methanation Turnover Numbers

Catalyst	Dispersion	k_0	E (kJ/mol)	a	b
JM1	0.78	1.43×10^9	118 ± 3	−0.76 ± 0.20	0.84 ± 0.20
JM4	0.16	1.09×10^8	101 ± 9	−0.71 ± 0.47	1.15 ± 0.45

TABLE 6

Methane Specific Activities: Comparison with Other Work at 101 kPa

Catalyst, % Ru on Al_2O_3	Dispersion	Temperature (°C)	H_2/CO	N_{CH_4} (10^{-3} s^{-1})	Reference
9.5	0.60	250	2/1	10.4	King (6)
1.25	0.44	250	2/1	19.5	King (6)
1.3	0.82	206	2/1	0.01	Kellner and Bell (4)
11	0.3	206	2/1	0.6	Kellner and Bell (4)
0.5	0.78	250	5/1	11	This work
0.5	0.16	250	5/1	38	This work

persions of 0.16 and 0.78. The data correspond to H_2/CO feed ratios of 5/1. The goodness of fit is shown in Fig. 6. Comparison of the methane TON obtained in the present investigation with values reported in the literature are given in Table 6. In all cases the methane TON increased with decreasing dispersion, indicative of the structure sensitivity of the methanation reaction. Furthermore, the values of the present investigation are in good agreement with those reported in the literature.

For reaction conditions ($H_2/CO < 3$) where the catalyst dispersion could not be measured directly by CO chemisorption, the correlations of Table 5 were used to predict the methane specific activity (for catalysts JM1 and JM4). The ratio of the measured CH_4 production rate per mole total Ru and the predicted methane specific activity, N_{c_1}, gave an estimate of the Ru dispersion. In addition, the higher hydrocarbon TON's were calculated from

$$N_{c_i} = (N_{c_1}/r_{c_1})r_{c_i}$$

or

$$N_{c_i} = k_0 \exp(-E/RT)P_{CO}^{a}P_{H_2}^{b}(r_{c_i}/r_{c_1}) \quad (2)$$

r_{c_i}/r_{c_1} is the ratio of the measured hydrocarbon (c_i) to methane rate per mole of (total) Ru.

With reference to Table 7 for the JM1 catalyst, the measured CH_4 production rate per mole total Ru was 16.0×10^{-4} mol (mol Ru)$^{-1}$ s^{-1} while the predicted CH_4 TON,

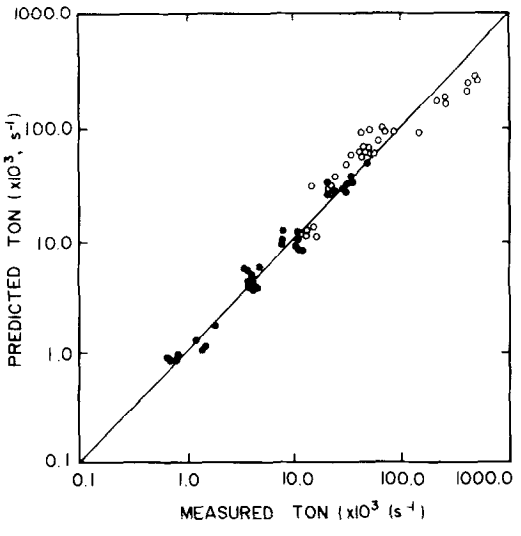

FIG. 6. Goodness of fit for methanation power law: (●) JM1 catalyst, (○) JM4 catalyst.

TABLE 7

Estimated Hydrocarbon Turnover Numbers

Hydrocarbon	TON = 10^{-4} s^{-1} at 235°C, 808 kPa, H_2/CO = 2.3, CO conv. 30%	
	Catalyst JM1, dispersion[a] = 0.78	Catalyst JM4, dispersion[a] = 0.16
C_1	24	186
C_2	2	15
C_3	4	37
C_4	3	31
C_5	3	34
C_6	2	23
C_7	1	17
C_8	0.9	13
C_9	0.6	6
C_{10}	0.3	7

[a] Ru dispersion of fresh catalyst.

calculated using the parameters for JM1 from Table 5, was 23.7×10^{-4} s^{-1}. Hence the estimated Ru dispersion (with carbonaceous deposits) is (16.0/23.7) = 0.68, the higher hydrocarbon TON's are $N_{c_i} = 23.7 \times 10^{-4}$ (r_{c_i}/r_{c_1}) s^{-1}, and for C_2, $r_{c_2}/r_{c_1} = 0.0802$ (measured), hence $N_{c_2} = 2 \times 10^{-4}$ s^{-1}.

The above technique was used to estimate TON's for the linear saturated hydrocarbons up to carbon No. 10, for a range of operating conditions, over catalysts JM1 and JM4. The parameter values k_0, E, a, and b in Eq. (2) are those given in Table 5 for the respective catalysts. Estimated TON's up to C_{10} are given in Table 7.

The data of Table 5 show that the parameters k_0 and E depend on the Ru dispersion, while the exponents a and b are not significantly different for catalysts JM1 and JM4, with fresh Ru catalyst dispersions of 0.78 and 0.16, respectively. During FT synthesis, Ru surface area decreases due to sintering as well as carbon deposition. The technique outlined above, corrects for loss of surface area due to carbon deposition but not for sintering which occurs during the course of the synthesis reaction. From Table 2, however, the latter effect would be expected to decrease Ru dispersion in the order of 20%. In view of the fivefold difference in fresh catalyst dispersions for catalysts JM1 and JM4, the error in assuming that the kinetic parameters of Tables 5 do not change significantly due to sintering during synthesis is, therefore, not expected to significantly affect the results of the present work.

The power rate law was also applied to the estimated TON's of the hydrocarbons, the results of which are given in Table 8 for the catalysts with unused dispersion of 0.78 and 0.16 (JM1 and JM4) up to carbon number 4. Some trends are noted from the data of Table 8. For both catalysts, the apparent activation energies decrease with increasing carbon number. Furthermore, for a particular hydrocarbon, the apparent activation energy decreased with Ru dispersion. The magnitudes of the H_2 and CO exponents increased with decreased Ru dispersion. In the present investigation, all the parameters were significant at the 95% level. The parameters are in good agreement with the data of Kellner and Bell (*5*) as shown in Table 9.

CONCLUSIONS

Sintering the 0.5% Ru/Al_2O_3 catalysts in air, significantly decreased the Ru dispersion and also affected the higher hydrocarbon selectivities as well as the olefinic content of the product. Increasing crystallite size results in an increase in both these quantities. The mass percent of the alcohol

TABLE 8

Power Rate Law Parameters for Hydrocarbon Turnover Number[a]

Hydrocarbon	Catalyst JM1, dispersion[b] = 0.78				Catalyst JM4, dispersion[b] = 0.16			
	k_{0i}	E_i[c]	a_i	b_i	k_{0i}	E_i[c]	a_i	b_i
C_2	7.42×10^9	137	−0.18	0.95	7.09×10^8	121	−1.54	1.47
C_3	3.49×10^5	93	−0.62	0.69	8.98×10^4	77	−1.48	2.07
C_4	1.61×10^4	79	−0.32	0.56	2.74×10^2	57	−1.24	1.77

[a] $N_{c_i} = k_{0i}\exp(-E_i/RT)P_{CO}^{a_i}P_{H_2}^{b_i}$.
[b] Ru dispersion of fresh catalyst.
[c] In kJ/mol.

TABLE 9

Hydrocarbon Power Rate Law Parameters: Comparison with Other Work

Hydrocarbon	Kellner and Bell (5), dispersion[a] = 0.6			This work, dispersion[a] = 0.78		
	E_i[b]	a_i	b_i	E_i[b]	a_i	b_i
C_1	117	−0.96	1.31	118	−0.96	0.84
C_2	105	−0.85	1.45	137	−0.18	0.95
C_3	75	−0.49	1.37	93	−0.62	0.69
C_4	79	−0.46	1.21	79	−0.32	0.56

[a] Ru dispersion of fresh catalyst.
[b] In kJ/mol.

appearing in the product is largely independent of the Ru crystallite size.

Comparison of CH_4 specific activities for the various catalyst crystallite sizes, together with the CH_4 activation energies, leads to the conclusion that the methanation reaction is structure sensitive over supported Ru.

The specific activities for the individual hydrocarbons, estimated indirectly, increase with a decrease in Ru dispersion. The parameters of the power rate law for the individual hydrocarbons (up to C_4) show, generally, a decreased activation energy and increased magnitude of the CO and H_2 exponents with decreased dispersion. These results are indicative of a structure sensitive reaction.

ACKNOWLEDGMENTS

The authors are grateful to Johnson Mattey Research Centre (U.K.) for financial assistance and for supplying the catalysts. Mr. J. Jenkins of JMRC did most of the catalyst characterization. The useful discussion with Professor Michel Boudart at Stanford University is acknowledged. Kevin Smith also acknowledges the Post-Graduate Research Fellowship sponsored by AECI (South Africa).

REFERENCES

1. Anderson, R. B., *in* "Catalysis" (P. H. Emmett, Ed.), Vol. IV. Reinhold, New York, 1965.
2. Everson, R. C., Woodburn, E. T., and Kirk, A. R. M., *J. Catal.* **53,** 186 (1978).
3. Kellner, C. S., and Bell, A. T., *J. Catal.* **71,** 288 (1981).
4. Kellner, C. S., and Bell, A. T., *J. Catal.* **75,** 251 (1982).
5. Kellner, C. S., and Bell, A. T., *J. Catal.* **70,** 418 (1981).
6. King, D. L., *J. Catal.* **51,** 386 (1978).
7. Smith, K. J., M.Sc. thesis. University of Natal, Durban, R.S.A., 1979.
8. Storch, H. H., Golumbic, N., and Anderson, R. B., "The Fischer–Tropsch and Related Synthesis." Wiley, New York, 1951.
9. Vannice, M. A., *J. Catal.* **37,** 449 (1975).
10. Dalla Betta, R. A., Piken, A. G., and Shelef, M., *J. Catal.* **40,** 173 (1975).
11. Everson, R. C., Mulay, L. N., Mahajan, O. P., and Walker, P. L., *J. Chem. Technol. Biotechnol.* **29,** 1 (1979).
12. Brisk, M. L., Day, R. L., Jones, M., and Warren, J. B., *Trans. Inst. Chem. Eng.* **46,** T3 (1968).
13. Carberry, J. J., *Ind. Eng. Chem. Process. Des. Dev.* **56,** 36 (1964).
14. Renouprez, A., Huang-Van, C., and Compagnon, P. A., *J. Catal.* **34,** 411 (1974).
15. Butt, J. B., *AIChE J* **22**(1), 1 (1976).
16. Anderson, R. B., *J. Catal.* **55,** 114 (1978).
17. Henrici-Olivé, G., and Olivé, S., *Angew. Chem. Int. Eng. Ed.* **15,** 3 (1976).